

# NIOZ3: Independent Temperature Sensors Sampling Yearlong Data at a Rate of 1 Hz

Hans van Haren, Martin Laan, Dirk-Jurjen Buijsman, Louis Gostiaux, Marck G. Smit, and Edwin Keijzer

**Abstract**—Some 110 independent sensors form the NIOZ3-thermistor “string” to study waves in the ocean interior sampling at a rate of 1 Hz during at least one year. The string operates without connecting cables between the newly designed sensors, which are programmed and synchronized via induction. The accuracy of previous custom-made high-sampling rate thermistor strings is maintained, being better than 1 mK. This is demonstrated here using data from three recent field trials, two above seamounts and one in the ocean interior that occasionally show vigorous (nonlinear) internal wave motions.

**Index Terms**—Deep-ocean temperature sensor, high precision, inductive communication, minimal power consumption, observations of waves in ocean interior.

## I. INTRODUCTION

**T**O continue monitoring ocean interior temperature variations, we have constructed a new temperature sensor that can sample at a rate of 1 Hz during a period of 1.5 y with accuracy better than 1 mK. This instrument “NIOZ3” can be used as an individual standalone sensor. Its internal clock is imprecise by about 1 min/y. When two or more sensors are mounted on a conductive cable they are synchronized to a single standard clock via induction. In principle, an infinite amount of sensors can thus be reached at arbitrary mutual distances tested up to 300 m away from the “synchronizer.” The same method of induction is used to communicate with the sensors, of which currently 110 have been built. Here, we present the first sea trials above seamounts and from the open ocean.

The instrumentation is built to specifically study waves and large scale turbulent motions that may contribute to mixing and redistribution of material in the ocean. Linear, freely propagating “internal waves” have periods  $T$  larger than the buoyancy period  $T_N = 2\pi/N$ ,  $N = (-g d \ln \rho / dz)^{1/2}$  the buoy-

Manuscript received May 30, 2008; accepted April 09, 2009. Current version published August 05, 2009. The construction and deployment of NIOZ3 were supported by The Netherlands organization for the advancement of scientific research (NWO) under Investment Grants “Oceanographic Equipment” and “LOCO.”

**Associate Editor: J. F. Lynch.**

H. van Haren is with the Department of Physical Oceanography, Royal Netherlands Institute for Sea Research (NIOZ), 1790 AB Den Burg, The Netherlands (e-mail: hans.van.haren@nioz.nl).

M. Laan, M. G. Smit, and E. Keijzer are with Department of Marine Technology Electronics, Royal Netherlands Institute for Sea Research (NIOZ), 1790 AB Den Burg, The Netherlands (e-mail: martin.laan@nioz.nl; marck.smit@nioz.nl; edwin.keijzer@nioz.nl).

D.-J. Buijsman was with the Royal Netherlands Institute for Sea Research (NIOZ), 1790 AB Den Burg, The Netherlands. He is now with Fiber SenSys LLC, Hillsboro, OR 97124 USA (e-mail: dirkjurjen@hotmail.com).

L. Gostiaux is with the Coriolis/LEGI, University of Grenoble, 38000 Grenoble, France (e-mail: louis.gostiaux@hmg.inpg.fr).

Color versions of one or more of the figures in this paper are available online at <http://ieeexplore.ieee.org>.

Digital Object Identifier 10.1109/JOE.2009.2021237

TABLE I  
SPECIFICATION OF THE NIOZ HIGH-SAMPLING RATE  
THERMISTOR STRING MODEL 3 (NIOZ3)

Range	[-10, 50]°C, approximately
Accuracy	<1.0 mK
Sensor response time ( $\tau$ )	0.25 s
Sampling frequency	adjustable: 0 – 2 Hz
Signal to noise ratio	0.1 mK
Power supply	1 Lithium C-cell battery
Battery life at 1 Hz	2 years
Battery capacity	6 x 10 <sup>7</sup> samples
Optical download rate	6000 samples/s
Number of sensors	variable
Distance between sensors	flexible
Current max string length	300 m (cascading is possible)
Depth rating	6000 m
Sensor dimensions	L = 175 mm; $\varnothing$ = 33 mm
Material pressure housing	Titanium grade V

ancy frequency,  $g$  the acceleration of gravity,  $d$  the total derivative,  $\ln$  the natural logarithm,  $z$  the vertical coordinate, and  $\rho$  the density. Deeper than 100 m from the surface, typical values are  $T > T_N = 1000$ – $3000$  s. On the other hand, internal wave periods are restricted by the rotation of the earth, as  $T < T_f = 2\pi/f$ ,  $f = 2\Omega \sin \varphi$  the vertical component of the earth rotational vector  $\Omega$  at latitude  $\varphi$ , when  $N \gg f$ . At midlatitudes,  $T_f = 50\,000$ – $86\,400$  s (14–24 h).

However, linear, purely sinusoidal waves do not transport material, but they can do so after steepening by becoming nonlinear, eventually leading to breaking. The processes of nonlinearity and breaking are induced following wave–wave and wave–current interactions, e.g., of small scale waves of frequency  $N$  interacting with vertical current shear setup by large scale waves of frequency  $f$ . These processes are most dramatic above sloping topography such as seamounts where they can dominate sediment resuspension and transport up the slope [1].

To monitor nonlinear waves and breaking one has to resolve time scales down to 1 s and vertical scales  $O(1$  m), much shorter than the buoyancy scales. Previously, such short scales have been resolved using accurate temperature sensors near the surface, but mainly towed from a ship (e.g., [2]) or from a device that floats freely for a period of a few days [3]. Near the bottom, at great depths, few 1-mK accurate instruments have resolved the above scales over short periods of a day [4] up to two weeks [5]. The newly designed NIOZ3 is versatile and can be used at slopes as well as in the open ocean down to 6000 m.

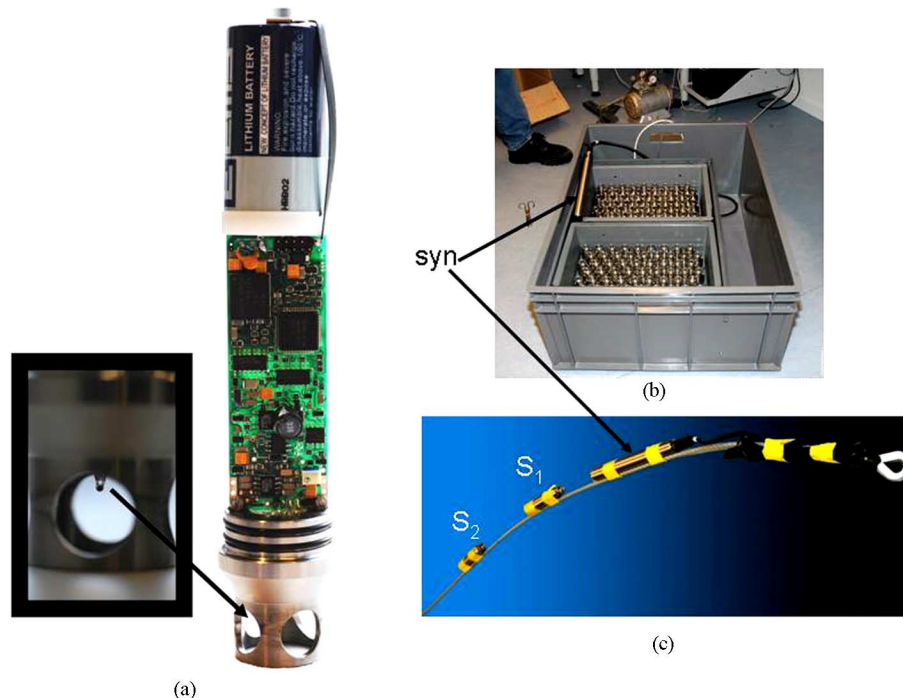


Fig. 1. Some specific NIOZ3 pictures. (a) Enlarged sensor tip (left) and one side of sensor electronics with Lithium C-cell battery (right). (b) Box with two cases including 110 sensors and one synchronizer on top. In the large box, an inductive magnetic field can be generated, for communication and programming purposes. (c) Nylon-coated 9.5-mm steel mooring cable with end connection electrically wired to synchronizer (syn), which is followed up the cable by two NIOZ3 sensors (S1 and S2). Photo courtesy: B. Aggenbach.

## II. TECHNICAL DETAILS

The core of the NIOZ3 temperature sensor is the embedding of its thermistor in a Wien (bridge) oscillator, just like NIOZ1 sensors [6]. In comparison with NIOZ1, a higher frequency oscillator is used, 48 MHz, and only one thermistor per sensor is used instead of two. The result is a fairly accurate sensor, estimated to be better than 0.5 mK, of which the precise value basically depends on the calibration. Its resolution is much higher ( $\sim 0.04$  mK, or  $\sim 4 \times 10^{-5} \text{ }^\circ\text{C}$ ). The main progress of NIOZ3 over NIOZ2 [5] and NIOZ1 is its much longer endurance of about 1.5 y instead of 15 d while sampling at a rate of 1 Hz (see Table I for details of NIOZ3). This progress is achieved together with a few novel changes in the setup of the instrument.

NIOZ3 has no connecting cables between the sensors, which are therefore standalone and independent (Fig. 1). The titanium housing contains all electronics, the sensors' program, a 256-MB memory flashcard, and a single C-cell battery. It can only be opened on one side. The cap is sealed with two O-rings and holds the single glass-embedded thermistor that is led through the cap via two small O-rings. All electronic components are designed for minimum power consumption. This includes the internal clock, which therefore is rather inaccurate by about 1 s/week. An additional clock is installed in a separate housing that can also house a pressure sensor. This "synchronizer" is used for two main purposes.

First, it sends a synchronizing clock pulse through a conducting cable or frame at user-installable time intervals of typically 5–10 h. In this way, all deviations of the separate clocks are

lined up to a single standard. Second, it interfaces the communication between a computer and sensors. Each sensor contains two coils mounted perpendicular to each other so that they can receive signals inductively from any transverse direction and up to a distance of 0.3 m from the conducting cable. As a result, when mounted to a 0.009-m diameter nylon-coated steel mooring line or put in a box near a magnetic field creator as during the programming, the sensors can receive communication and synchronization signals. Inductive communication is one-way and for the return–response, an light-emitting diode (LED) is used behind the glass opening of the sensor tip. Particular sequences of LED flashings tell the user about correct or false transmission codes and synchronization.

Shipborne conductivity temperature with depth (CTD) observations just before instrument deployment is used to calibrate the sensors, besides establishing the large scale interior density stratification expressed in buoyancy frequency  $N$  and the temperature–density anomaly relationship. This *in situ* calibration is required at approximately the same pressure level where the sensors will be moored, but foremost a very fast ( $< 3$  h) manner of obtaining a 1-mK relative accuracy. The well-calibrated and accurate Seabird-911 CTD temperature sensor is used as a reference to find homogeneous layers that are numerous in the ocean. Such layers alternating with thin stratified layers are created in part by internal waves, our principal subject of the study. After this independent calibration of sensors, a remaining constant due to a weak influence of pressure on the thermistor is added during postprocessing via "autocalibration," an automated procedure. This procedure corrects for the irregularities in the time-averaged temperature profile, which is sup-

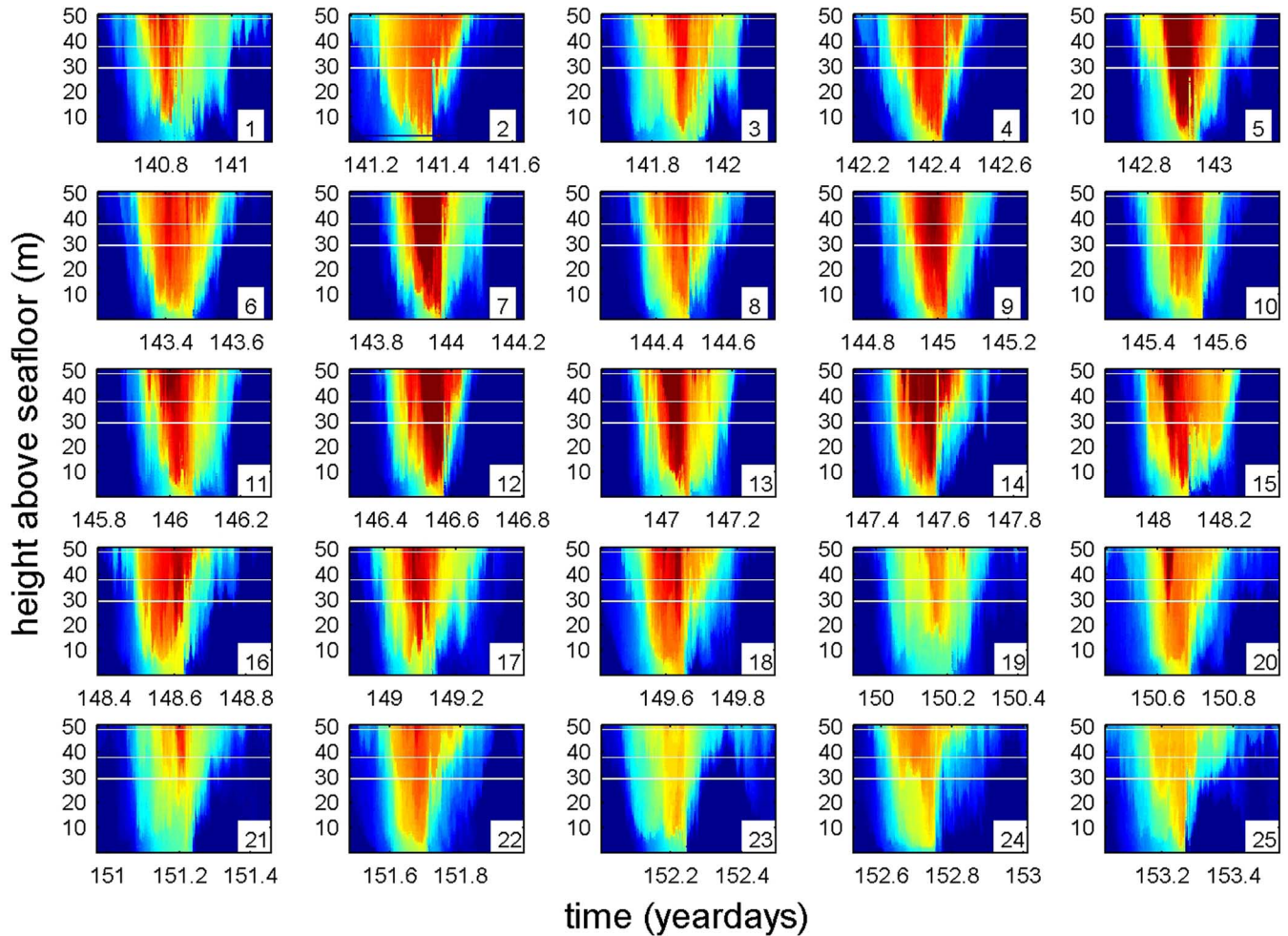


Fig. 2. First 25 semidiurnal lunar tidal ( $M_2$ ; 12.42 h) periods of depth-time series of temperature measured using NIOZ3 up to 50 mab (meters above the bottom) near the top of Great Meteor Seamount. Temperature ranges from 12.3 °C to 14.1 °C.

posed to be smooth, to guarantee the 1-mK absolute<sup>1</sup> calibration of the sensors. The same procedure corrects for any failures in reception of the synchronization pulse.

### III. FIELD TRIALS

#### A. Exercise 1: 19-d Deployment Above Great Meteor Seamount

The sloping sides, having angles  $\theta$  to the vertical, of Great Meteor Seamount (GMS), a 4000-m-high guyot in the Canary Basin, North Atlantic Ocean, are generally much larger than the critical slope  $\alpha$  for internal tide gravity wave generation or reflection:  $|\alpha| = \sin^{-1}[\frac{(\sigma^2 - f^2)}{(N^2 - \sigma^2)}]^{0.5} \approx 1.1^\circ \ll \theta$  for  $\sigma = M_2$  and  $N = 50$  cycles per day (cpd), the typical stratification locally near the mooring. This is still approximately the case for the slope at 550 m near the top of GMS, where locally  $\theta \approx 3.9^\circ \pm 0.1^\circ$  as measured by tilt sensors in a current meter and in an upward looking 300-kHz acoustic Doppler current profiler (ADCP), both mounted on a bottom lander frame in May–June 2006 (see Table II for mooring details). Attached

<sup>1</sup>We deliberately write “absolute calibration” to highlight the fact that the sensors not only have a relative accuracy of 1 mK, with an undefined constant to be added, but also record 1-mK temperature differences relative to each other. Nevertheless, this “absolute calibration” is not to be understood in terms of absolute temperature measurement with respect to the absolute zero.

TABLE II  
MOORING DETAILS OF NIOZ3(N3)-DEPLOYMENT TRIALS.  
THE “UNIT” mab DENOTES METERS ABOVE THE BOTTOM

Exercise #	1	2	3
Latitude	30° 00.052' N	00° 44.154' N	33° 00.010' N
Longitude	028° 18.802' W	039° 51.178' W	022° 04.841' W
Waterdepth	549 m	1150 m	5274 m
bottom slope	4°	20°	--
deployment	21-05-06	05-12-07	10-06-06
recovery	08-06-06	13-12-07	22-11-07
N3 sampling	1 Hz	1 Hz	1 Hz
N3 lowest	0.5 mab	0.6 mab	1522 m
N3 highest	50 mab	54 mab	1390 m
N3 #sensors	100	90	54
N3 distance	0.5 m	0.6 m	2.5 m
N3 synchro	18000 s	18000 s	18000 s

to the frame, 96 NIOZ3 were taped to a mooring cable at 0.5-m mutual distances. Additionally, four sensors were mounted on the frame at the same distance of 0.5 m between them. Tilt information of a current meter above NIOZ3 showed that the string did not move more than  $\sim 0.2$  m vertically and 3 m horizontally, despite current speeds up to  $0.55 \text{ m s}^{-1}$ .

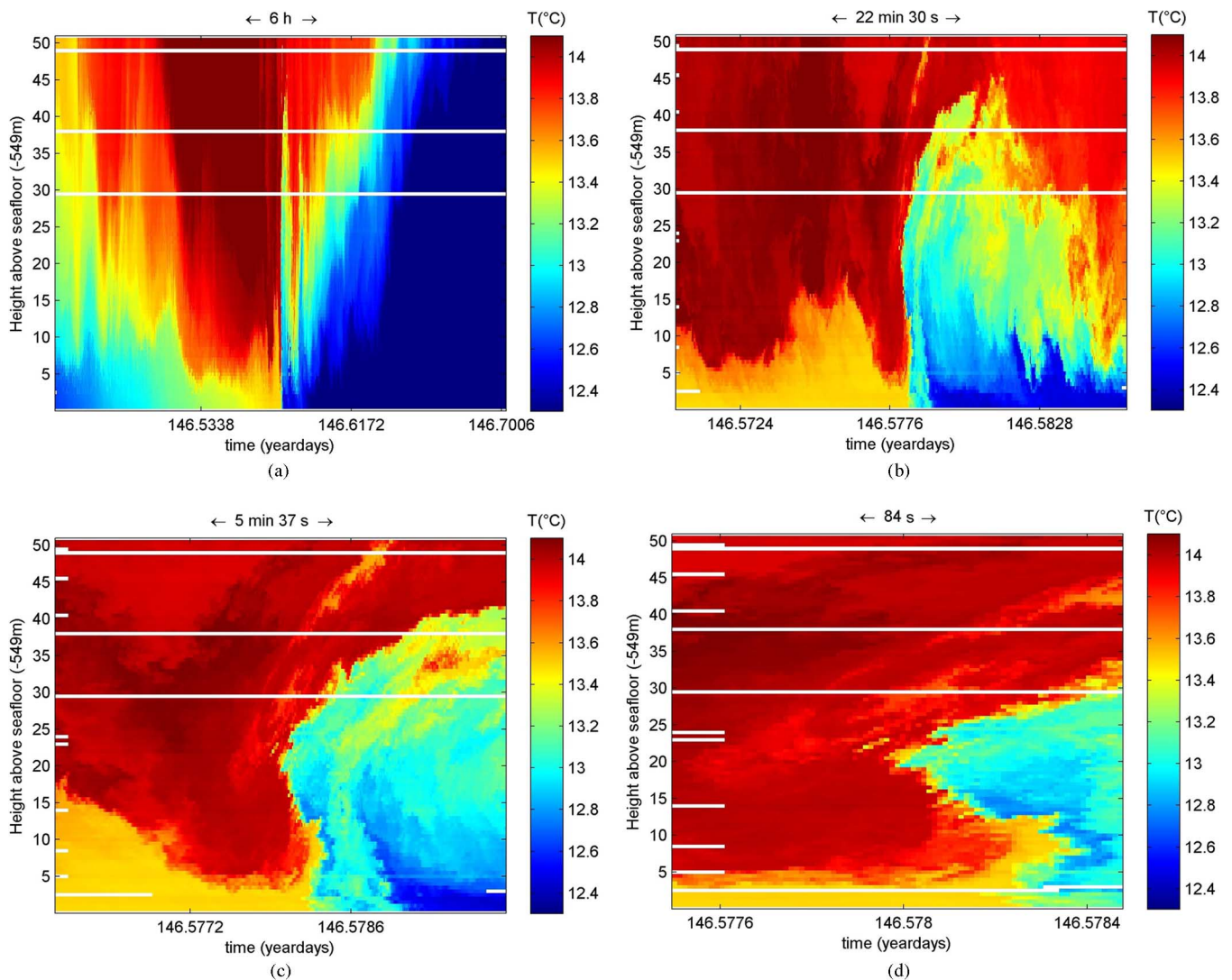


Fig. 3. Details from the 12th panel of Fig. 2, with increasing zoom on the cold-front.

The dominant temperature variations show a semidiurnal tidal periodicity in the bottom boundary layer (bbl) exceeding 50 mab (meters above the bottom), the range of the present temperature measurements (Fig. 2). However, the semidiurnal temperature variation is far from sinusoidal or linear wavelike. The warming phase is longer and more gradual, while the cooling phase commences abruptly. Furthermore, during none of the 37 semidiurnal tidal periods in the record, the bbl behaved the same in detail. These changes in detail are not associated with the spring-neap change with time, but due to changes in interior stratification and subinertial vorticity, thereby affecting the internal wave field approaching sloping bottoms. Likewise, the associated sediment resuspension as inferred from ADCP's echo intensity, or acoustic backscatter, is different for each of the individual strongly nonlinear upslope motions.

Zooming in more detail, NIOZ3 reveals details of a front (Fig. 3), similar in quality to that of NIOZ2 [5] but over much larger time spans and with very few failing sensors. During this first NIOZ3 trial, only three sensors failed and another eight missed the first synchronization pulse (see the white short lines on the left-hand side of the panel). Note that data in any panel are

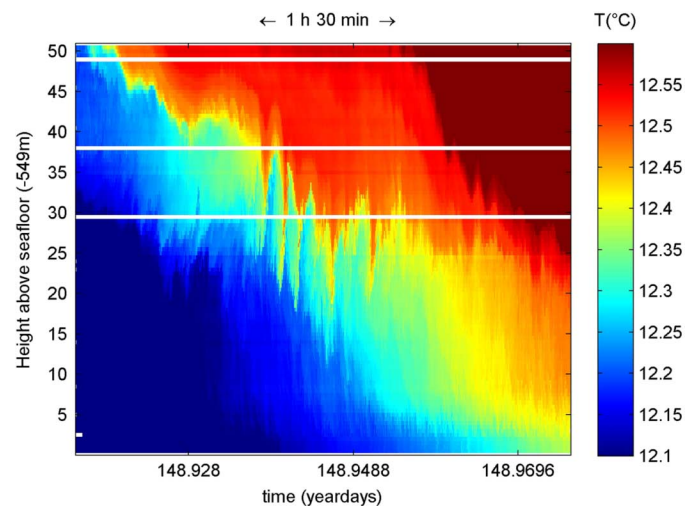


Fig. 4. Detail from the 17th panel of Fig. 2 showing turbulent "fingers" during the warming phase of the tide. The scale is different from the one in Fig. 2.

unsmoothed, raw, and that only in the two most detailed panels all data are represented by individual pixels. In the other panels,

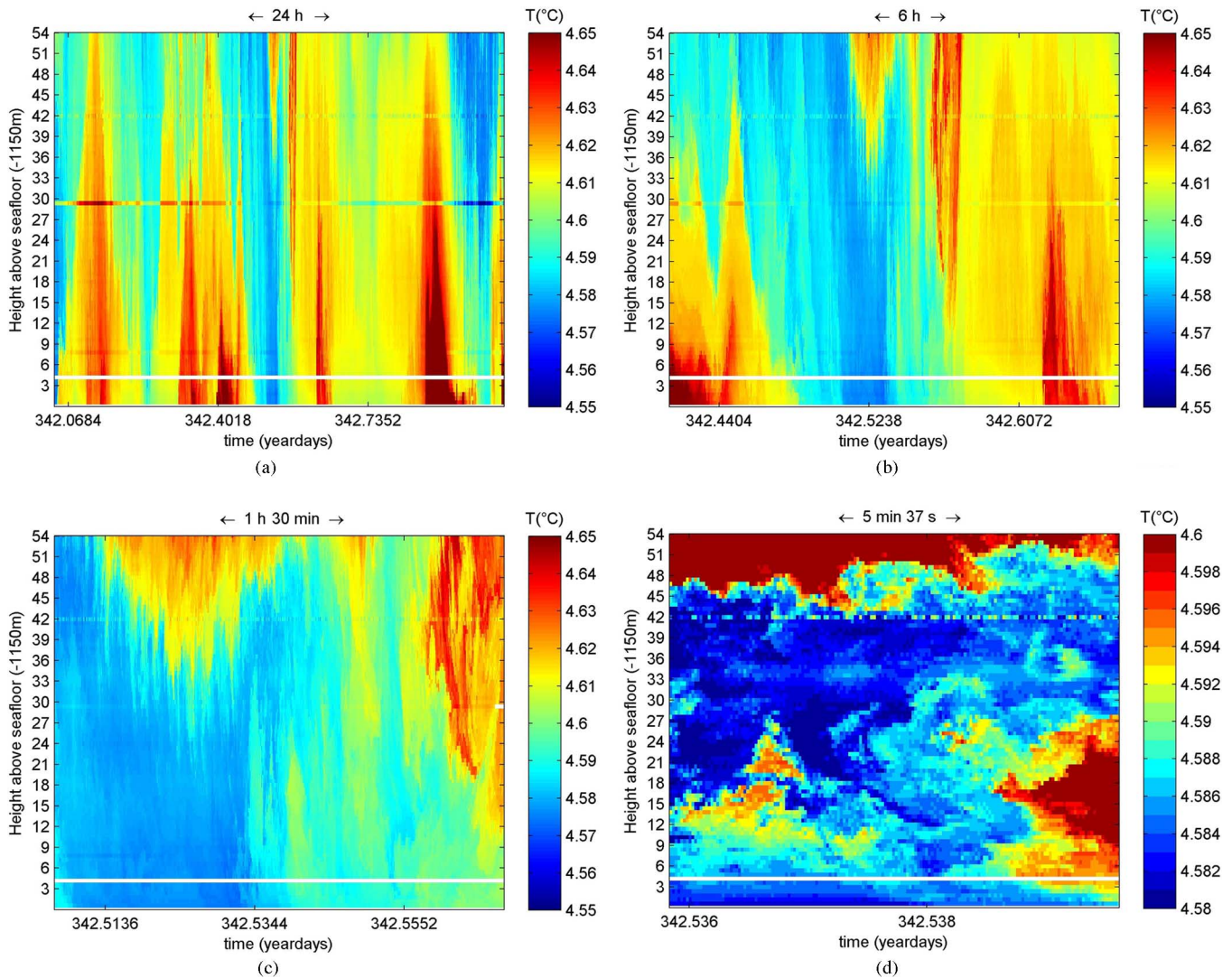


Fig. 5. Depth-time series of temperature measured up to 50 mab above the upper ridge of a seamount in the equatorial Ceará Basin. Window zoom increases from 1 d to 5 min and 37 s. Note the reduction in scale for the last, most detailed panel.

data points are skipped without interpolation as they are not resolved at 300 dpi in standard journal image size. The frontal details reveal overturning, but also the instruments' capability of measuring the temperature accurately in this area as revealed from the smallest structures that remain coherent over at least a few sensors. Such smallest structures vary over time scales  $O(10\text{ s})$ , which is much faster than the buoyancy period  $T_N$ , even when the latter is computed across thin ( $\Delta z = 1\text{ m}$ ), strongly stratified layers  $T_{N,\text{max}} = O(10^2 - 10^3\text{ s})$ . Hence, these structures are not representing freely propagating internal waves. Recall that each sensor is operating completely independently.

The variation of observed details is also revealed during passages of other phases of the tide, e.g., during the downslope propagating warming phase, when thin “finger” clouds are advected by the tidal flow (Fig. 4). These have a vertical extent of typically 5–10 m and last 30–60 s, again much shorter than the smallest buoyancy period. They reach very near the bottom and they seem associated with rather vigorous shear and convective processes, as they resemble sinking under atmospheric clouds. Some develop as regular Kelvin–Helmholtz-type instabilities. More precise analysis will follow in the near future. As with the

large and most vigorous fronts of the upslope motion, the fingers' form and intensity vary greatly between the tidal periods. This can be seen in a 180-s movie of two out of 19 days of the record.<sup>2</sup>

This record shows that NIOZ3 can monitor rapid temperature variations down to scales of 1 s and 0.5 m. As the temperature variation in this area was rather high, a few degrees Celsius, its full capacity of precise temperature measurements was yet to be tested. This was done using a near-equatorial mooring described below.

### B. Exercise 2: 8-d Mooring With Very Small Temperature Variations

In November 2007, we deployed 90 NIOZ3 sensors, 87 on a mooring cable and three on a bottom-lander frame, at 0.6-m mutual distances, in otherwise the same configuration as in Section III-A, near the top of an equatorial seamount in Ceará Basin to the north of Brazil (see Table II for mooring details).

<sup>2</sup>See: <http://www.nioz-hst.com/spip.php?article3>

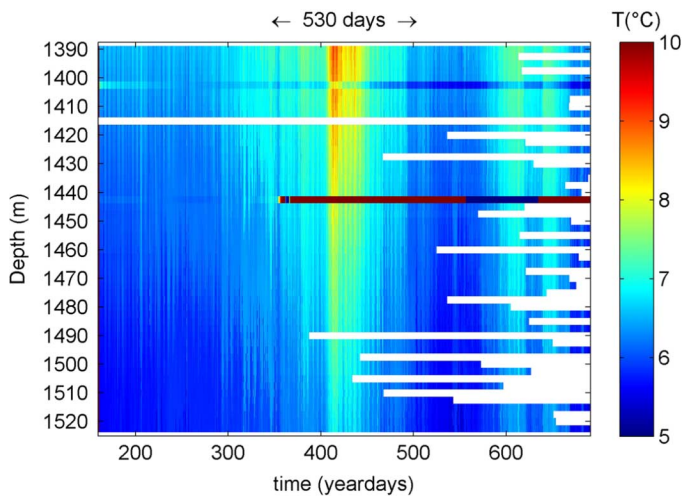


Fig. 6. Overview of 1.5 y of temperature data measured using NIOZ3 sensors sampling at a rate of 1 Hz in the open Canary Basin.

The bottom lander was located at 1150 m, about 200 m below the seamount's summit. Unfortunately, the lander dropped off its ridge to a steep bottom slope of  $\theta \approx 20^\circ \pm 1^\circ$ . As a result, the ADCP was shut down most of the time as it operates beams that are slanted at the same angle to the vertical coordinate as the estimated mean slope. The current meters in the frame and above NIOZ3 operated normally, showing speeds regularly approaching  $0.25 \text{ m s}^{-1}$ , half the size of those near the top of GMS, except once up to  $0.42 \text{ m s}^{-1}$ .

During this deployment, only two NIOZ3 sensors failed and none missed a synchronization pulse. The others showed (ir)regular bursts of moderately vigorous motions. In the Ceara Basin, the main variation is not semidiurnal tidal, but merely fourth-diurnal, which also reaches very near the bottom [Fig. 5(a)]. Recall that the lowest sensor is attached to the frame at 0.6 mab. A most striking difference with the GMS data is the reversal of the temperatures with depth: upslope motions are associated with warming. It is due to a local inverse temperature structure, which must be compensated by salinity for stability. This has been verified using shipborne CTD profiles at stations nearby, which show a salinity increase with depth between 800 and 1300 m that is sufficiently large to compensate for the relatively weak temperature inversion between these depths. Otherwise, the asymmetric periodic motions are similar to those observed above GMS. The main difference is the temperature range, which is two orders of magnitude smaller in the Ceara Basin.

Zooming in detail [Fig. 5(b) and (c)] and down to the instruments full resolution [Fig. 5(d)] demonstrates an absolute accuracy  $< 1 \text{ mK}$ . In the latter panel of largest detail, the scale range of  $0.02 \text{ }^\circ\text{C}$  ensures a different tone is used for every 1 mK. Clearly, these tones are well resolved in coherent structures of several meters in height lasting  $O(10 \text{ s})$ . As in this case the temperature is not the only contributor to density variations, it must be considered as a tracer rather than being used for diapycnal turbulent diffusivity estimates. Nonetheless, this picture does show the vigorous turbulent overturning associated with bottom boundary layer processes, at least in a qualitative way.

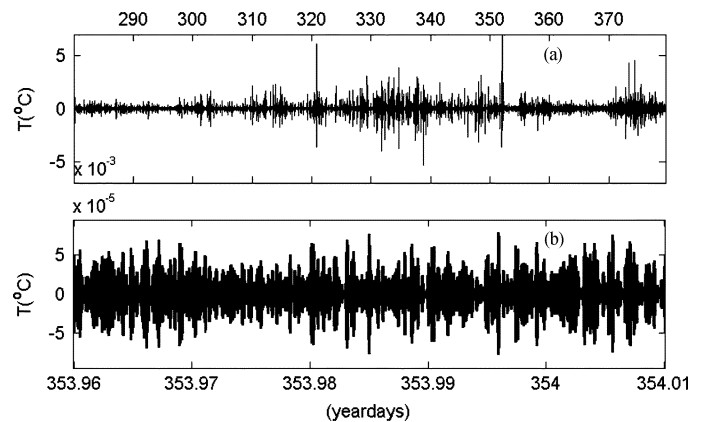


Fig. 7. High-pass filtered NIOZ3 data from sensor 1 (1390 m) in the Canary Basin. The filter cut-off is at 0.4 Hz. (a) Time series of 100 days. (b) Detail showing very low instrumental noise levels (note the different vertical scale compared to (a)).

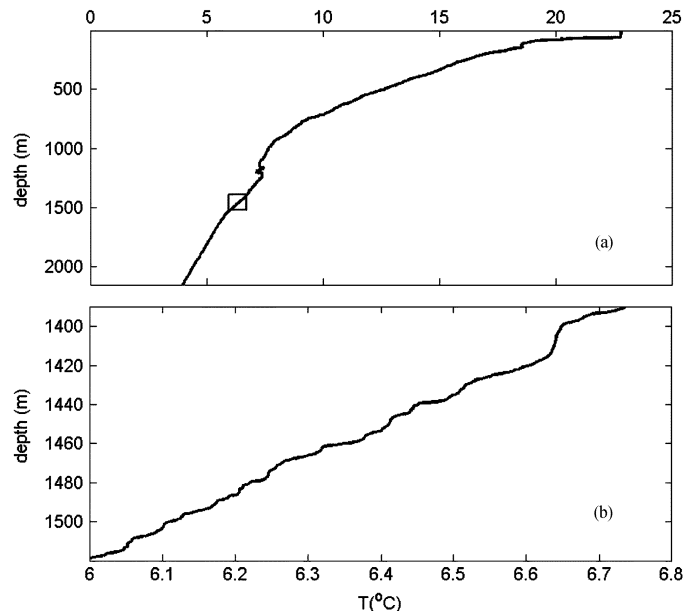


Fig. 8. CTD-temperature profile obtained near NIOZ3 in the Canary Basin during mooring recovery. (a) Upper 2000 m, with rectangle indicating the range of NIOZ3. (b) Detail from rectangle in (a).

### C. Final Exam: 18-Months Mooring in the Canary Basin

To learn more about open-ocean internal wave motions, their variability on the longer "climatic" time scales and whether they are as nonlinear as near-bottom motions, NIOZ3 sensors were deployed for 1.5 y while sampling at a rate of 1 Hz. This thermistor string consisted of 54 sensors at 2.5-m intervals and was mounted directly below the top buoy of a 3800-m-long mooring to the West of Madeira in the Canary Basin (CB) between May 2006 and November 2007 (see Table II for details). Pressure and tilt sensor information showed  $< 1.5^\circ$  tilt angle and excursions across  $< 1.2 \text{ m}$  in the vertical direction and  $< 100 \text{ m}$  in the horizontal direction. Thus, mooring motion did not affect the temperature observations.

The result of this first 1.5-y deployment of accurate NIOZ3 sensors running at 1 Hz is not so bad (Fig. 6). Initially, only

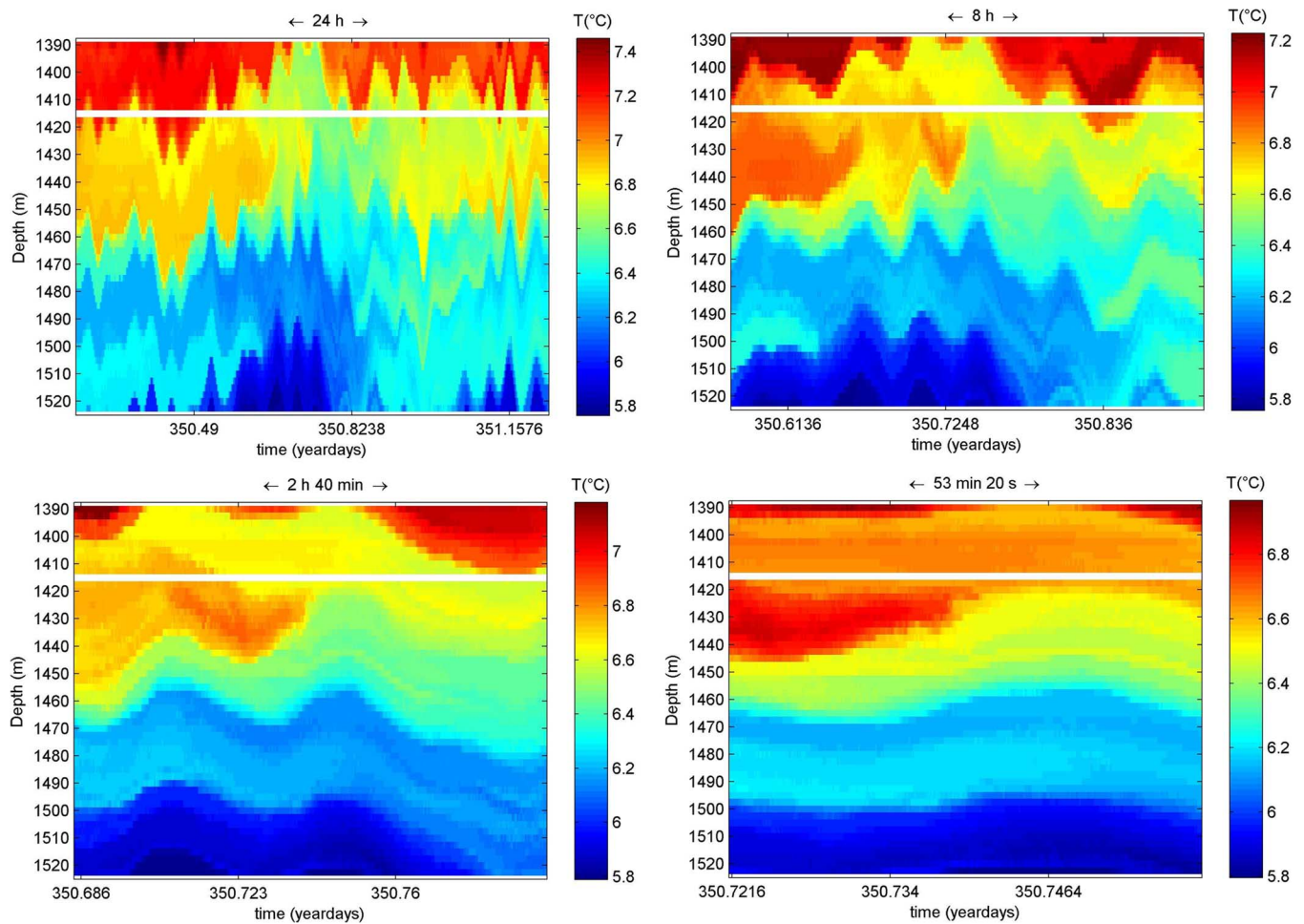


Fig. 9. Depth-time series of temperature measured between 1390 and 1522 m for an arbitrary day in the Canary Basin, with increasing zoom to 53 minutes and 20 seconds.

one, from day 350 onwards two, sensor failed. Some 18 sensors continued accurate sampling the entire period of 530 d. The remaining sensors stopped, mainly in the second half of the record, but this is all attributable to a known battery problem. This problem is solved now.

The noise level in these data is occasionally extremely low, down to about  $50 \mu\text{K}$ , or  $5 \times 10^{-5} \text{ }^\circ\text{C}$  (Fig. 7). These values confirm the instrumental noise level. The periods with higher apparent noise level contain high-frequency natural turbulent motions. A seasonal cycle seems to occur in these motions, but during first analysis, we could not find coherence between these motions and large scale energy sources, such as tides or atmospheric disturbances. This requires further study.

From hydrographic CTD observations during the deployment and previous cruises it was known that NIOZ3 could reach through the lower part of Mediterranean outflow water, which commonly propagates in large eddies (Meddies). Nevertheless, the large temperature variations up to  $5 \text{ }^\circ\text{C}$  difference across this relatively small vertical range of 132.5 m are unexpected, when considering a single CTD profile (Fig. 8). It is clear when such a Meddy passes, e.g., between 400 and 450 days (Fig. 6). In addition to this large scale structure are fine lines across

almost the entire range of sensors that represent smaller scale eddies and groups of internal waves.

In more detail, the vertical coherence of motions is striking (Fig. 9). On the larger internal wave scale, semidiurnal tidal motions are visible. But also much higher frequency motions up to the buoyancy frequency show vertical coherence across 100 m, to the first order. Weaker and stronger stratified layers move up and down, more or less simultaneously. This layering is typical for the open ocean [Fig. 8(b)]. Partially, these layers are due to convective mixing processes, and partially they are due to internal wave straining, the dominant process yet being unknown.

Perhaps, due to the sensor separation  $>1 \text{ m}$ , less detailed internal wave breaking is observed. On the other hand, this is open ocean and the motions are more representing quasi-linear waves, compared to the areas above seamounts. Nevertheless, interleaving layers are also displaced with the same regularity as other, step-like stratification (Fig. 9). It shows that temperature can be used as a tracer to monitor internal wave motions, even though salinity differences are dominating stability.<sup>3</sup>

<sup>3</sup>The rich variability of the ocean interior in permanent motion, with wave heights of typically  $O(10 \text{ m})$ , is best shown in video available at [http://www.dailymotion.com/relevance/search/internal%2Bwaves/video/x4coxi\\_3in131\\_tech](http://www.dailymotion.com/relevance/search/internal%2Bwaves/video/x4coxi_3in131_tech). See also <http://www.nioz-hst.com/spip.php?article9>

#### IV. FUTURE DEVELOPMENTS

Although the NIOZ3 temperature sensor matches the requirements set, revealing oceanic internal wave motions to the detail of large turbulent scales over periods longer than a year, it still offers room for improvements. In the near future, we plan NIOZ4, which includes:

- a smaller sensor, having a diameter of 0.023 m, about two-thirds of the diameter of the NIOZ3-sensor and running on a single AA-cell while sampling at 1 Hz for a year;
- sensor pressure independence, which should make calibration much easier and no longer necessary for each individual deployment at different pressure levels;
- conductivity, for direct estimates of density anomalies;
- differential pressure sensor mounted on the synchronizer for monitoring baroclinic (internal wave) pressure variations, an important dynamic variable but difficult to measure.

#### ACKNOWLEDGMENT

The authors would like to thank the crew of the *R/V Pelagia* for deployment and recovery of the moorings. They would also like to thank R. Groenewegen, B. Koster, and T. Hillebrand for enjoyable discussions on NIOZ-temperature sensor instrumentation.

#### REFERENCES

- [1] P. Hosegood, J. Bonnin, and H. van Haren, "Solibore-induced sediment resuspension in the Faeroe-Shetland channel," *Geophys. Res. Lett.*, vol. 31, L09301, 2004, DOI:10.1029/2004GL019544.
- [2] G. O. Marmorino, "Observations of small-scale mixing processes in the seasonal thermocline. Part II: Wave breaking," *J. Phys. Oceanogr.*, vol. 17, pp. 1348–1355, 1987.
- [3] J. L. Cairns, "Internal wave measurements from a mid-water float," *J. Geophys. Res.*, vol. 80, pp. 299–306, 1975.
- [4] S. A. Thorpe, "Current and temperature variability on the continental slope," *Phil. Trans. R. Soc. Lond.*, vol. A 323, pp. 471–517, 1987.
- [5] H. van Haren, R. Groenewegen, M. Laan, and B. Koster, "High sampling rate thermistor string observations at the slope of great meteor seamount," *Ocean Sci.*, vol. 1, pp. 17–28, 2005, SRef-ID: 1812-0792/os/2005-1-17.
- [6] H. van Haren, R. Groenewegen, M. Laan, and B. Koster, "A fast and accurate thermistor string," *J. Atmos. Ocean. Technol.*, vol. 18, pp. 256–265, 2001.



**Hans van Haren** received the Ph.D. degree in geophysics (physical oceanography) from the University of Utrecht, Utrecht, The Netherlands, in 1990.

Currently, he is Senior Scientist within the Department of Physical Oceanography, Royal Netherlands Institute for Sea Research (NIOZ), Den Burg, The Netherlands.



**Martin Laan** completed secondary education in electronics.

Currently, he is a Senior Electro-Technician at the Department of Marine Technology Electronics, Royal Netherlands Institute for Sea Research (NIOZ), Den Burg, The Netherlands. He is specialized in analog and digital systems.



**Dirk-Jurjen Buijsman** completed higher education in electronics and information technology.

He was temporarily affiliated with Royal Netherlands Institute for Sea Research (NIOZ), Den Burg, The Netherlands, as imbedded Software Engineer. Currently, he is with Fiber SenSys LLC, Hillsboro, OR.



**Louis Gostiaux** received the Ph.D. degree in physics from Ecole Normale Supérieure (ENS), Laboratoire de Physique, Lyon, France, in 2006.

Following his postdoctoral stay at Royal Netherlands Institute for Sea Research (NIOZ), Den Burg, The Netherlands, currently he runs the rotating platform Coriolis of the University of Grenoble, Grenoble, France.



**Marck G. Smit** received the M.Sc. degree in marine engineering from the Faculty of Maritime Technology, Delft University of Technology, Delft, The Netherlands, in 1987.

Currently, he is Head of the Department of Marine Technology Electronics, Royal Netherlands Institute for Sea Research (NIOZ), Den Burg, The Netherlands.



**Edwin Keijzer** completed secondary education in mechanical engineering.

Currently, he is Fine-Mechanics Instrument Maker at the Department of Marine Technology Electronics, Royal Netherlands Institute for Sea Research (NIOZ), Den Burg, The Netherlands.